Front. Phys., 2014, 9(1): 120–127
DOI 10.1007/s11467-013-0365-1

RESEARCH ARTICLE

Firing rates of coupled noisy excitable elements

Shuai Liu[1,2], **Zhi-Wei He**[1,2], **Meng Zhan**[1,†]

[1] *Wuhan Center for Magnetic Resonance, State Key Laboratory of Magnetic Resonance and Atomic and Molecular Physics, Wuhan Institute of Physics and Mathematics, Chinese Academy of Sciences, Wuhan 430071, China*

[2] *University of the Chinese Academy of Sciences, Beijing 100049, China*

Corresponding author. E-mail: [†] *zhanmeng@wipm.ac.cn*

Received May 10, 2013; accepted June 24, 2013

The dynamics of coupled excitable FitzHugh–Nagumo systems under external noisy driving is studied. Different from most of previous work focusing on the noise-induced regularity in the framework of coherence resonance, here the average frequency (or firing rate) of coupled excitable elements is of much more concern. We find that (i) their frequencies first increase and then decrease with the increase of the coupling, and there is a clear crossover from a rush increase to a smooth increase with the increase of noise strength, and (ii) for nonidentical cases, all elements transit to an identical frequency simultaneously only after a certain coupling strength is achieved. These first-increase-then-decrease non-monotonic frequency behavior and isochronous frequency synchronization are believed to be two basic behaviors in coupled noisy excitable systems.

Keywords coupled excitable elements, firing rate, noise, coherence resonance

PACS numbers 05.45.Xt, 05.40.Ca, 87.19.lm

1 Introduction

The collective behaviors of coupled nonlinear elements [1–3] are of great significance for our understanding of many dynamical processes in biological systems, such as the circadian rhythms showing that many living organisms synchronize to the day-night cycle [4, 5] and the coherent beats synchronously created by the intestinal muscles in heart [6]. A clear fact is that all these collective behaviors are created by a network of more or less similar coupled systems, not a single one. Thus, it is clear that the theoretical study of coupled nonlinear oscillators in the nonlinear dynamics field can provide a powerful and helpful means for these problems. On the other hand, for many realistic systems, the effects of various fluctuations, such as the influences of intrinsic (intracellular), extrinsic (intercellular) and external (environmental) noises in multicellular systems, are always unavoidable. Quite opposite to the idea that noise can only be a nuisance, with the development of the theory of stochastic resonance [7–12], researchers have already found that noise may even induce coherent motion and have many positive roles in biological functions, for example, regulation in genetic networks, maintenance of the quantitative individuality of cells, noise-driven divergence of cell fates, noise-induced amplification of signals and so on. Indeed, many other regularity effects induced by noise or other types of disorder have been reported and intensively studied, including stochastic resonance without an external periodic force [13], coherence resonance in excitable systems [14], array-enhanced stochastic resonance [15], array-enhanced coherence resonance [16, 17], vibrational resonance [18–21], diversity-induced resonance [22–24], ghost resonance [25, 26], etc. Therefore, it is only natural to see that the study of noise effect on coupled nonlinear systems has continued being a hot topic for several decades.

In a very recent paper [27], the collective dynamics of coupled excitable FitzHugh–Nagumo (FHN) elements in the presence of noise was studied. In particular, the authors focused on how the average frequency (or firing rate) changes with the variation of the coupling strength, and they found an unexpected peak in the frequency variation before reaching synchronization. This model study has well reproduced the unexpected peak in the variation of the beating rates observed in cultured cardiac cells experiments. Following their work, in the present paper we will further study the dynamics in coupled excitable noisy FHN elements for different noise strengths. We find that actually there are two different types of frequency enhancement, corresponding to the large and

small noises, respectively. In addition, we find that all non-identical elements transit to the synchronous state at the same value of coupling. This feature may fundamentally differ from our familiar concept of frequency synchronization in coupled nonlinear oscillators, where bifurcation trees are generally observed. Finally, a qualitative explanation is provided to establish a whole physical picture for these findings.

2 Single excitable noisy FHN

First, let us start from the classical work of Pikovsky and Kurths for the finding of coherence resonance [14] by studying a single noise-driven FHN model,

$$\begin{aligned} \varepsilon\dot{x} &= x - x^3/3 - y \\ \dot{y} &= x + a + \xi(t) \end{aligned} \tag{1}$$

where ε is small allowing one to separate the x and y variables for the fast and slow motions, respectively, and another system parameter a characterizes the system dynamics: if $|a| > 1$, the system has only one stable fixed point ($x = -a, y = -a + a^3/3$), and otherwise for $|a| < 1$, it shows a limit cycle. For $|a|$ slightly larger than one ($|a| \gtrsim 1$), the system is excitable, namely, only a sufficiently large perturbation can make the system deviate from the fixed point and exhibit a large near-limit-cycle excursion. In addition, $\xi(t)$ is a Gaussian white noise: $\langle \xi(t)\xi(t')\rangle = D\delta(t-t')$, with D being the noise strength. Though the FHN model is only a prototype for an excitable system (e.g., neuron), it does perfectly catch the essential character of excitability of neuron with x denoting the membrane potential and y a recovery variable.

Here D governs the system dynamics if other system parameters ε and a are fixed: for $|a| \gtrsim 1$ and $D = 0$, the system is quiescent, whereas for $D \neq 0$, different patterns of pulse trains (or spike trains) can be generated. Note that these pulse trains are induced and sustained by noise. It was found that for both small and large D, the noise-induced oscillations appear to be rather irregular, while for moderate noise relatively coherent oscillations can be observed [14]. This noise-induced regularity (termed coherence resonance) has been well characterized quantitatively by the normalized fluctuations of pulse durations (or coefficient of variation of pulse trains)

$$R = \frac{\sqrt{Var}(t_p)}{\langle t_p \rangle} \tag{2}$$

where t_p denotes the interval (or called interspike interval) starting at the end of one pulse to the beginning of the next pulse plus the pulse duration, and the bracket $\langle\ \ \rangle$ indicates an average over large numbers for sufficiently long time. As an example, the non-monotonic resonant behavior of R as a function of D is shown in both the semi-log plot and regular plot in Figs. 1(a) and (b); here $\varepsilon = 0.01$ and $a = 1.05$ are the same as in Ref. [14]. This regularity induced by noise may also be demonstrated by other quantities, such as the characteristic correlation time and the signal-to-noise ratio.

In this work, we are interested in the variation of the average frequency (or firing rate) of the pulse trains, which can be simply defined by

$$f = \frac{1}{\langle t_p \rangle} \tag{3}$$

In the literature, the firing rate may be more specifically termed as spike-count rate, which may be easily obtained by counting the average number of spikes that appears in a sole trial [28]. In Fig. 1 the value of f has also been calculated, showing a clear monotonic increase. One may find that a rush increase exists for very small D, and after a certain D, f turns out slowly increasing with D. Below we will see that this feature may contribute to the different behaviors of firing rate in coupled excitable systems under different noise strengths.

The phenomenon of coherence resonance has been well explained by the different noise dependencies of the activation time t_a and the excursion time t_e [10, 14, 29]. $t_p = t_a + t_e$. The activation time t_a is the (waiting) time needed to excite the system from the stable fixed point, and it obeys approximately a Poissonian process with strong dependence on D. In contrast, the excursion time t_e is the time needed to return from the excited state to the fixed point, and it only weakly depends on D. For small D, $t_a \propto \exp(const \times D^{-1})$ according to the Kramers rate [30], and it decreases rapidly with D; this scale relation has been confirmed by our numerical result if $D < 5 \times 10^{-4}$. Under this situation, $t_a >> t_e$ and $t_p \approx t_a$. For large D, $t_a \to 0$ and $t_p \approx t_e$. On the assumption of statistical independence between the two times, the squared coefficient of variation can be subdivided into two independent terms and it shows a minimum at intermediate noise strength, indicative of the occurrence of coherence resonance, as shown in the plot of R versus D in Fig. 1. We may also use the above knowledge to intuitively understand the monotonic increase of f and especially the fast increase component for extremely small D: as D increases from zero, t_a and, accordingly, t_p decreases rapidly since $t_p \approx t_a$, while for larger D, t_e dominates and t_p becomes saturate with the change of D since $t_p \approx t_e$.

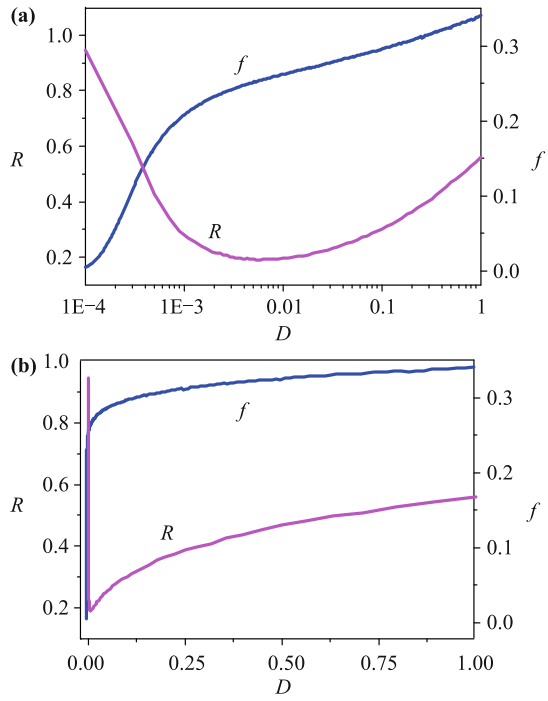

Fig. 1 **(a)** and **(b)** The coefficient of variation of pulse trains R and the firing rate f in a single FHN element as a function of noise strength D in a semi-log plot and regular plot, respectively. $\varepsilon = 0.01$ and $a = 1.05$. Coherence resonance for the noise-induced dynamical regularity of a noisy excitable element can be well characterized by the non-monotonic behavior of R vs. D. In contrast, f monotonically increases from zero.

3 Coupled excitable noisy FHNs

Next consider the following coupled system consisting of N FHN noisy excitable elements, described by [16, 27]

$$\begin{aligned} \varepsilon_i \dot{x}_i &= x_i - x_i^3/3 - y_i + g \sum_j{}' (x_j - x_i) \\ \dot{y}_i &= x_i + a_i + \xi_i(t), \quad i = 1, 2, \cdots, N \end{aligned} \tag{4}$$

where g represents the (electronic) coupling strength (here we assume g capable of being either positive or negative, which corresponds to attractive or repulsive coupling, respectively.). $\sum'$ denotes the summation over connected neighbors, and here we consider only the nearest-neighboring connection. Thus, for a one-dimensional (1D) ring, the coupling term is $g(x_{i+1} + x_{i-1} - 2x_i)$, while for a 2D lattice, the coupling term should be modified accordingly. For both the 1D and 2D cases, we choose the periodic boundary conditions. Here the noises for all excitable elements are uncorrelated and their strengths are taken to be the same: $\langle \xi_i(t)\xi_j(t')\rangle = D\delta_{ij}\delta(t - t')$. The parameter ε_i is always chosen to be identical for all coupled elements, i.e., $\varepsilon_i = 0.01$ for all i's, while a_i's are set to be slightly larger than one and changeable for different i's.

As the first step, we consider the simplest case for identical a and $N = 2$. Figure 2(a) shows the results for different noise strengths; here $a_1 = a_2 = 1.05$. $f_1 = f_2 = f$, and the coupling terms in Eqs. (4) become $g(x_2 - x_1)$ and $g(x_1 - x_2)$ for $i = 1$ and 2, respectively. From bottom to top, the curves correspond to four different D's: $D = 0.001, 0.01, 0.1$, and 1, respectively. Clearly for the attractive couplings ($g > 0$), all curves show a non-monotonic behavior: they first climb and damp with further increasing coupling. However, comparing these curves, we do find some difference between them: for small D, there is a rush increase for small g, while for large D, only a smooth increase exists. This difference can be contrasted to the common damping behavior under large g. To take a closer view of their disparity, we zoom in these curves on the small coupling part in Figs. 2(b) and (c) for $D = 0.001$ and $D = 1$, respectively. They have not only confirmed the recent finding of frequency enhancement in Ref. [27], but also shown richer behavior than what researchers previously thought. Additionally for the repulsive coupling ($g < 0$), f monotonically increases with g, and the deviation from this for small D is also obvious.

To characterize these different types of frequency enhancement and especially illustrate how they change with D in detail, we may define the local maximum value of the curve of f vs. g in the positive, right part ($g > 0$) as f_+ [as shown in Fig. 2(b)] and its corresponding value of g as g_+, accordingly f_- and g_- the negative, left part of f vs. g for $g < 0$, and f_0 at $g = 0$, and calculate their values for different D's; the results are shown in Fig. 3. In Fig. 3(a), g_+ starts climbing from zero for small D and increases rapidly for larger D, but contrarily, it seems that g_- jumps from a small constant to another large constant around $D \approx 10^{-2}$. From Fig. 3(b), we find that all f_+, f_- and f_0 monotonically increase with D, both f_+ and f_0 start from zero for small D, and f_- approaches to the value of f_0 with further increasing D. These curves well indicate the appearance of the small valley shown in Fig. 2(b) and its vanishing over a certain threshold ($D_c \approx 0.174$) [the vertical arrow in Fig. 3(b)]. Therefore, two different types of frequency enhancement [including the hard and soft ones, shown in Figs. 2(b) and (c), respectively] and their mutual transformation exist without any ambiguity.

In order to test the generality of these findings, Fig. 4 illustrates several examples for other parameters and system sizes. Two coupled nonidentical elements are treated and their corresponding firing rates are exhibited in Figs. 4(a) and (b), respectively. $a_1 = 1.05$ and $a_2 = 1.10$. Again for different noise intensities, two types of frequency enhancement for small and large D appear.

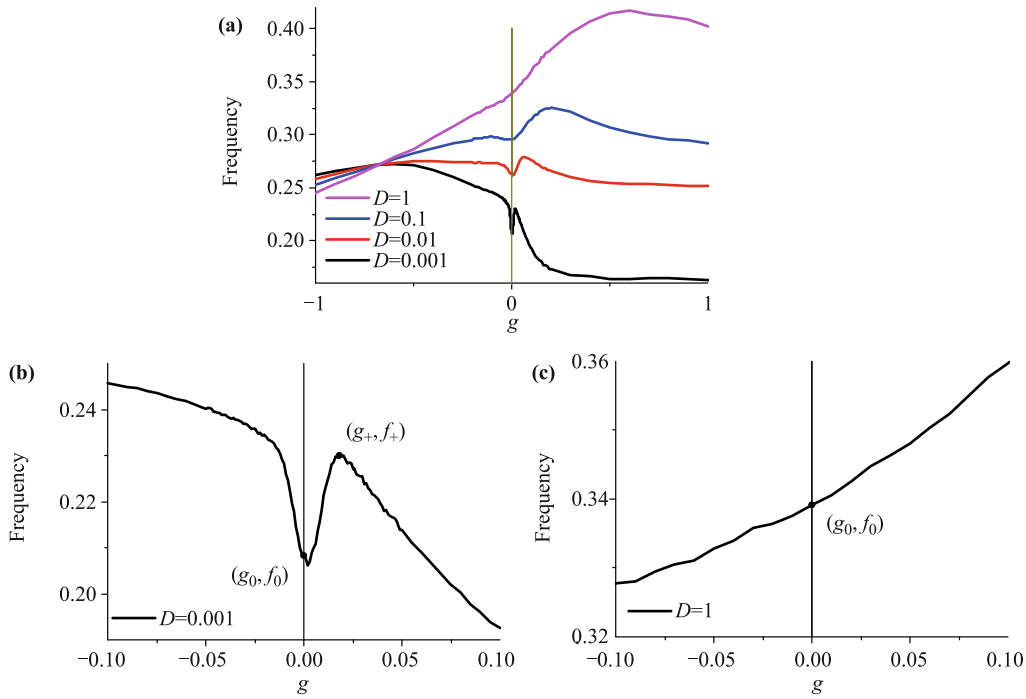

Fig. 2 **(a)** The dependence of the average frequencies (firing rates) of coupled noisy excitable elements on coupling g for different D's. If we focus on the attractive coupling ($g > 0$) part, as D increases from bottom to top, there are two different types of frequency enhancement (a rush increase for small D and a slow increase for large D). $N = 2$ and $a_1 = a_2 = 1.05$. **(b, c)** The magnifications of the frequency curves around $g \approx 0$ for two different D's: $D = 0.001$ and $D = 1$, respectively. In (b), a small valley for small D should contribute to the rush increase of frequency enhancement.

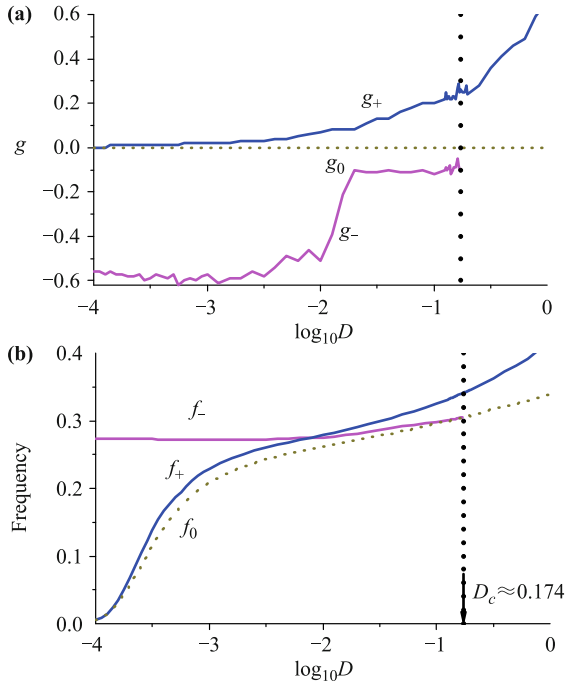

Fig. 3 **(a, b)** The dependence of g_+, g_-, g_0, f_+, f_-, and f_0 on D, indicative of a clear change for the average frequency from a rush increase to a slow increase at $D_c \approx 0.174$ (the vertical arrow). Here g_+ (g_-) is defined as the local maximum value of the right (left) part of frequency curve of f vs. g for $g > 0$ ($g < 0$) [as shown in Fig. 2(b)]. Its corresponding frequency is denoted by f_+ (f_-). Correspondingly, $g_0 = 0$ and f_0 is the frequency at $g = 0$. For more details, see texts and the schematic show in Fig. 2.

In Fig. 4(a), for $D = 0.001$, a magnification of the small region around $g = 0$ also shows a small drop, which might not be as apparent as its counterpart in Fig. 4(b). This effect may come from the fact that the element 1 is more excitable than the element 2 ($a_2 > a_1$). In addition, two other cases for a ring of $N = 100$ and a 20×20 2D lattice are given in Figs. 4(c) and (d), respectively, which again show the similar pattern; here $a_i = 1.05$, identical for all sites in both cases and the average frequencies for all elements are plotted.

We are interested in not only how these coupled elements change their firing rates with the coupling, but also their relationship. It is notable that for the identical case, though all firing rates change with the coupling, they always keep the same between each other. To this end, in Fig. 5 we give several examples for coupled nonidentical systems. In Figs. 5(a)–(c), $N = 3$ with different D's and a_i's considered. In Fig. 5(d), $N = 10$ with random a_i's chosen. Based on these extensive numerical calculations, clearly all these elements not only show frequency enhancement at intermediate coupling prior to the synchronization, but also transit to the synchronization simultaneously at exactly the same coupling strength. We may call it *isochronous synchronization*, which has been found to hold for all kinds of exhausted numerical test for other parameters and even larger N.

In the study of an assembly of nearest-neighbor

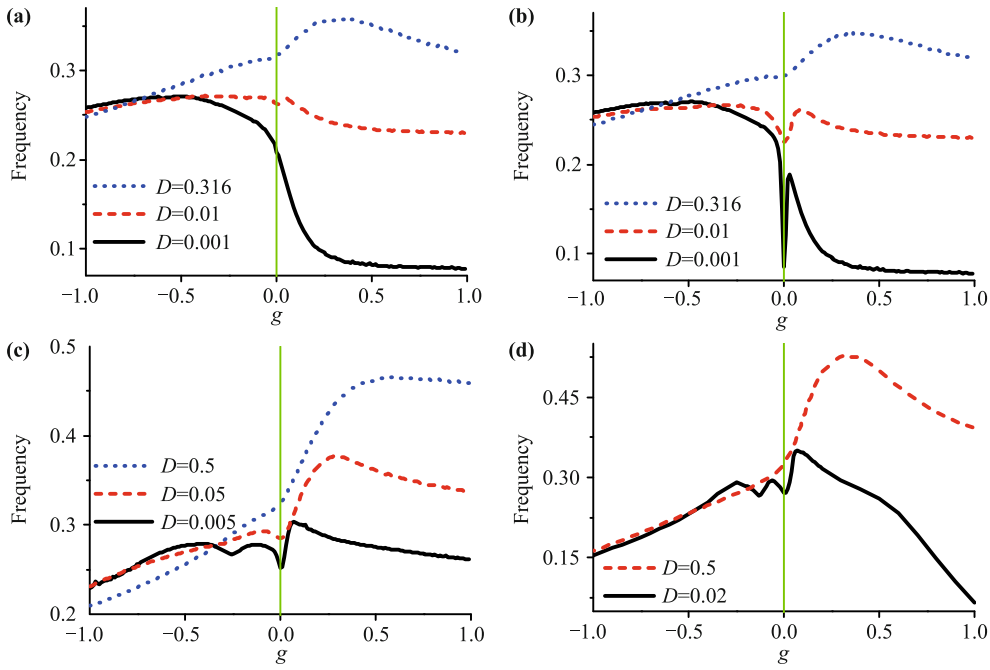

Fig. 4 The generality of frequency enhancement demonstrated by different cases: **(a, b)** $N = 2$, $a_1 = 1.05$ and $a_2 = 1.10$; **(c)** a near-neighbor coupled ring with $N = 100$ and $a_i = 1.05$ for all elements; and **(d)** a 20×20 lattice with $a_i = 1.05$ for all elements. In (a) and (b), the frequencies for elements 1 and 2 are plotted, respectively, whereas, in (c) and (d), the average frequencies for all elements are plotted. The parameter ε_i is always chosen to be identical for all coupled elements, i.e., $\varepsilon_i = 0.01$ for all i's.

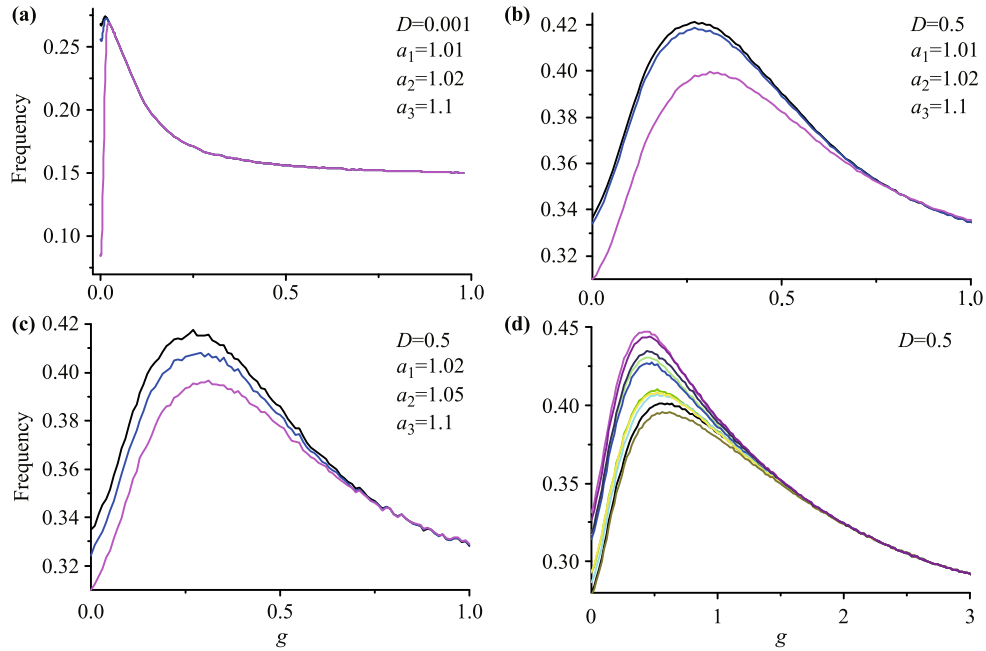

Fig. 5 The generality of isochronous synchronization demonstrated by different cases: **(a)** $N = 3, D = 0.001, a_1 = 1.01, a_2 = 1.02, a_3 = 1.1$; **(b)** $N = 3, D = 0.5, a_1 = 1.01, a_2 = 1.02, a_3 = 1.1$; **(c)** $N = 3, D = 0.5, a_1 = 1.02, a_2 = 1.05, a_3 = 1.1$; and **(d)** $N = 10$ and $D = 0.5$ with a_i randomly chosen within $[1.01, 1.21]$.

coupled limit-cycle oscillators, which can be theoretically described by the model of coupled Kuramoto phase oscillators [31–34], we are quite familiar with the general scenario to frequency synchronization for how each oscillator changes its frequency and transits to a common synchronous frequency. In such a scenario, generally the frequency of any oscillator can only lie between the maximum and the minimum of the intrinsic frequencies of

the elements, and thus the frequency (enhancement) out of the bound of the original frequencies is unusual. In addition, as coupling increases, any two adjacent oscillators (or adjacent clusters of oscillators) with close frequencies can be easily synchronized and show a larger synchronous cluster, and thus generally a tree of synchronization from small to large clusters (and finally only one biggest cluster) with the increase of coupling is observable [32–34]. Clearly here the frequency enhancement and the isochronous synchronization without subbifurcation and tree structure, which have been found in coupled noisy excitable elements, are fundamentally different from those in coupled limit-cycle oscillators. They might come from their distinctive origin of oscillation: noise-induced oscillation.

4 Qualitative physical picture

Below we attempt to understand these peculiar behaviors in a qualitative manner, though the whole systems dynamics is very complicated. Since the dynamics of single excitable element in the presence of noise is clear: the noise intensity should be high enough to overcome the threshold and produce a near-limit-cycle oscillation (spike), it might be easy to start from investigating how the coupling influences this behavior. For this purpose, we present the schematic shows for different types of coupling (either attractive or repulsive coupling) in Fig. 6. The simplest case $N = 2$ is considered. Clearly in the presence of attractive coupling in Fig. 6(a), the element 1 (solid circle), which stays at the quiescent state, is pulled by a force from the element 2 (open circle). As a result, it becomes easier for element 1 to overcome the threshold and be excited, and the direct outputs are that the activation time t_a becomes shorter and its average frequency increases. This is consistent with the extensive experimental observations that the number of spikes and further the firing rate of a neuron always increase with an effective stimulus for the neuron. On the contrary, if the repulsive coupling is considered [Fig. 6(b)], it will produce a frequency-attenuation effect. Based on these analyses, the monotonic increase for both $g > 0$ and $g < 0$ shown in Fig. 2(c) should be quite natural. In addition, the unusual behavior for small D has to come from the rush variation of f discovered in Fig. 1, and under this situation ($|g| \ll 1$), the noise-effect becomes dominant over the coupling-effect and produces a roughly symmetrical effect for both positive and negative g in Fig. 2(b).

Below let us focus on the attractive coupling. In Fig. 7(a), the spike trains of coupled excitable elements are

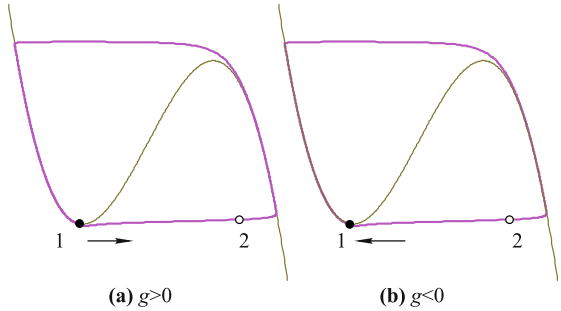

Fig. 6 Schematic show for the different bulk behaviors (frequency-enhancement and frequency-attenuation) induced by the attractive ($g > 0$) **(a)** and repulsive ($g < 0$) **(b)** couplings, respectively.

schematically shown. Again only $N = 2$ is considered. In the absence of coupling, the spikes (black vertical lines) of two elements are independent and both obey approximately a Poissonian process. With the (attractive) coupling added on, a direct effect is that element 1 will act with its spikes added on element 2's, and vice versa, as shown by the dashed vertical lines. We may define the probability of this direct adding effect due to the interaction as $\eta (0 \leqslant \eta \leqslant 1)$, and assume that η is proportional to the scaled coupling, namely, $\eta = g/g_{syn}$, with g_{syn} used to denote the critical coupling strength for synchronization. Based on the definition of firing rate in Eq. (3), a direct effect is the increase of frequency due to the increased number of spikes, and quantitatively we have

$$\begin{aligned} f_1(g) &= f_1 + \eta f_2 \\ f_2(g) &= f_2 + \eta f_1 \end{aligned} \tag{5}$$

where $f_1(g)$ and $f_2(g)$ denote the frequencies under coupling g for sites 1 and 2, respectively, and f_1 and f_2 are the corresponding frequencies in the absence of coupling ($g = 0$). Their linear increase relations have been illustrated in Fig. 7(b). Note that here the x axis is for coupling g and the y axis is for frequency f.

Clearly above we consider only how the two spike trains are purely superimposed by the interaction and we do not consider how each spike train changes with the coupling. Actually with the increase of coupling, the spike trains should become more sparse, which will naturally decrease the frequency. Below let us see this competitive effect. For the analysis of the collective dynamics around the synchronization state (i.e., $x_1 = x_2 = \ldots = x_N$ and $y_1 = y_2 = \ldots = y_N$), we may denote $X = \langle x_i \rangle$ and $Y = \langle y_i \rangle$ as its global dynamics with $\langle\ \rangle$ representing the average over all coupled elements. From Eqs. (4), we have

$$\begin{aligned} \varepsilon \dot{X} &= X - X^3/3 - Y - r^2 X - \rho^3/3 \\ \dot{Y} &= X + a_0 + \xi(t)/\sqrt{N} \end{aligned} \tag{6}$$

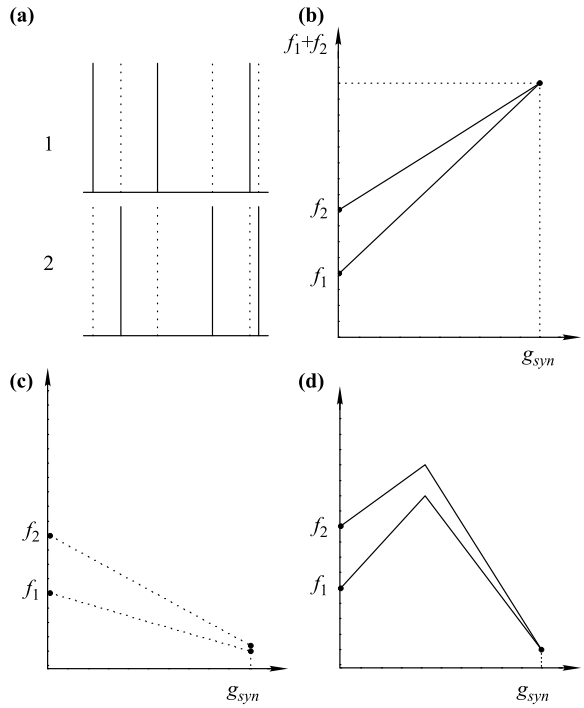

Fig. 7 Schematic show for the occurrences of the coupling-induced first-increase-then-decrease frequency variation, which is contributed by two opposite effects: the frequency enhancement in (a) and (b) and the frequency decrease in (c), and the isochronous frequency synchronization. In (b), (c), and (d), the x axis is for coupling g and the y axis is for frequency f. For more details, see the texts.

where $a_0 = \langle a_i \rangle$, and $r^2 = \langle (x_i - X)^2 \rangle$ and $\rho^3 = \langle (x_i - X)^3 \rangle$ for the high-order fluctuation around the global dynamics, which will vanish and be ignored if the global synchronization has been achieved. Here since the analysis is applied around the synchronization state, clearly the coupling strength term does not appear in the equations. Comparing these equations with Eqs. (1) for a single FHN, we may see that the coupled system after synchronization can be viewed as a single element subject to a white noise with scaled strength D/N. Note that similar analysis has been used by other researchers for other problems [16]. This relation can be expressed by

$$f(g_{syn}, D) = f(g = 0, D/N) \tag{7}$$

Combined with the fact of the monotonic increase of f vs. D in Fig. 1 for a single FHN, it definitely indicates that the average frequency should be greatly depressed by synchronization. Based on this point, the coupling-induced frequency attenuation (dashed line) is schematically shown in Fig. 7(c) with a reasonable linear estimation for the coupling g between $g = 0$ and $g = g_{syn}$.

Finally, these two opposite effects: coupling-induced frequency attenuation [Fig. 7(c)] and coupling-induced frequency enhancement [Fig. 7(b)] are combined and considered together in Fig. 7(d), which clearly shows the similar first-increase-then-decrease patterns in numerics as above. We also find that the isochronous synchronization occurs, exhibiting independent transition processes and a common synchronization threshold. Therefore, we believe that a reasonable qualitative picture in physics has been provided to explain the competitive dynamics in coupled excitable elements.

5 Conclusion

To summarize, we have found two key properties in coupled noisy excitable elements: the frequency enhancement and isochronous synchronization, which are believed to be the main characteristics of collective noisy dynamics induced by both noise and coupling. We have also classified two different types of frequency enhancement including hard rush and soft slow ones. The underlying possible mechanism for the non-monotonic frequency variation with the change of coupling is uncovered. All these findings have been extensively confirmed in numerics and supported by our qualitative analysis. Clearly the spike-count rate (or firing rate) of neuron is of great importance in the information encoding, decoding and even computing in neural network and brain network. They are relevant to many important and fundamental problems in the study of experimental and theoretical neuroscience, such as visually responsive neurons in the retina, lateral geniculate nucleus of the thalamus, and primary visual cortex [28]. Therefore, we expect that these interesting findings reported in the paper are capable of shedding an improved light on our understanding of biological complexity and complicated dynamics and functions in networks of neurons and noise-induced collective behaviors in excitable systems in general.

Acknowledgements This study was supported by the National Natural Science Foundation of China under Grant No. 11075202. We also thank the suggestions and comments of three referees very much.

References

1. A. T. Winfree, The Geometry of Biological Time, New York: Springer-Verlag, 1980
2. S. H. Strogatz, Nonlinear dynamics and chaos: With applications to physics, biology, chemistry, and engineering, Massachusetts: Perseus Books Publishing, 1994
3. A. Pikovsky, M. Rosenblum, and J. Kurths, Synchronization: A Universal Concept in Nonlinear Sciences, Cambridge: Cambridge University Press, 2001

4. T. B. Kepler, E. Marder, and L. F. Abbott, The effect of electrical coupling on the frequency of model neuronal oscillators, *Science*, 1990, 248(4951): 83
5. S. Yamaguchi, H. Isejima, T. Matsuo, R. Okura, K. Yagita, M. Kobayashi, and H. Okamura, Synchronization of cellular clocks in the suprachiasmatic nucleus, *Science*, 2003, 302(5649): 1408
6. M. R. Boyett, H. Honjo, and I. Kodama, The sinoatrial node, a heterogeneous pacemaker structure, *Cardiovasc. Res.*, 2000, 47(4): 658
7. R. Benzi, A. Sutera, and A. Vulpiani, The mechanism of stochastic resonance, *J. Phys. Math. Gen.*, 1981, 14(11): L453
8. L. Gammaitoni, P. Hanggi, P. Jung, and F. Marchesoni, Stochastic resonance, *Rev. Mod. Phys.*, 1998, 70(1): 223
9. T. Wellens, V. Shatokhin, and A. Buchleitner, Stochastic resonance, *Rep. Prog. Phys.*, 2004, 67(1): 45
10. B. Lindner, J. Garcia-Ojalvo, A. Neiman, and L. Schimansky-Geier, Effects of noise in excitable systems, *Phys. Rep.*, 2004, 392(6): 321
11. X. J. Zhang, H. Qian, and M. Qian, Stochastic theory of nonequilibrium steady states and its applications (Part I), *Phys. Rep.*, 2012, 510(1–2): 1
12. H. Ge, H. Qian, and M. Qian, Stochastic theory of nonequilibrium steady states. Part II: Applications in chemical biophysics, *Phys. Rep.*, 2012, 510(3): 87
13. G. Hu, T. Ditzinger, C. Z. Ning, and H. Haken, Two-dimensional vortex lattice melting, *Phys. Rev. Lett.*, 1993, 71(3): 807
14. A. S. Pikovsky and J. Kurths, Coherence resonance in a noise-driven excitable system, *Phys. Rev. Lett.*, 1997, 78(5): 775
15. J. F. Lindner, B. K. Meadows, W. L. Ditto, M. E. Inchiosa, and A. R. Bulsara, Array enhanced stochastic resonance and spatiotemporal synchronization, *Phys. Rev. Lett.*, 1995, 75(1): 3
16. B. Hu and C. S. Zhou, Phase synchronization in coupled nonidentical excitable systems and array-enhanced coherence resonance, *Phys. Rev. E*, 2000, 61(2): R1001
17. C. S. Zhou, J. Kurths, and B. Hu, Array-enhanced coherence resonance: Nontrivial effects of heterogeneity and spatial independence of noise, *Phys. Rev. Lett.*, 2001, 87(9): 098101
18. P. S. Landa and P. V. E. McClintock, Vibrational resonance, *J. Phys. Math. Gen.*, 2000, 33(45): L433
19. E. Ullner, A. Zaikin, J. Garcia-Ojalvo, R. Bascones, and J. Kurths, Vibrational resonance and vibrational propagation in excitable systems, *Phys. Lett. A*, 2003, 312(5–6): 348
20. C. G. Yao and M. Zhan, Signal transmission by vibrational resonance in one-way coupled bistable systems, *Phys. Rev. E*, 2010, 81(6): 061129
21. C. G. Yao, Y. Liu, and M. Zhan, Frequency-resonance-enhanced vibrational resonance in bistable systems, *Phys. Rev. E*, 2011, 83(6): 061122
22. C. J. Tessone, C. R. Mirasso, R. Toral, and J. D. Gunton, Diversity-induced resonance, *Phys. Rev. Lett.*, 2006, 97(19): 194101
23. S. F. Brandt, B. K. Dellen, and R. Wessel, Synchronization from disordered driving forces in arrays of coupled oscillators, *Phys. Rev. Lett.*, 2006, 96(3): 034104
24. C. G. Yao and M. Zhan, Simple electronic circuit model for diversity-induced resonance, *Phys. Lett. A*, 2010, 374(24): 2446
25. G. V. D. Sande, G. Verschaffelt, J. Danckaert, and C. R. Mirasso, *Phys. Rev. E*, 2005, 72: 016113
26. P. Balenzuela, J. Garcia-Ojalvo, E. Manjarrez, L. Martinez, and C. R. Mirasso, Ghost resonance in a pool of heterogeneous neurons, *Biosystems*, 2007, 89(1–3): 166
27. W. Y. Chiang, P. Y. Lai, and C. K. Chan, Frequency enhancement in coupled noisy excitable elements, *Phys. Rev. Lett.*, 2011, 106(25): 254102
28. P. Dayan and L. F. Abbott, Theoretical Neuroscience: Computational and Mathematical Modeling of Neural Systems, Massachusetts: The MIT Press, 2001
29. K. Pakdaman, S. Tanabe, and T. Shimokawa, Coherence resonance and discharge time reliability in neurons and neuronal models, *Neural Netw.*, 2001, 14(6–7): 895
30. H. Z. Risken, The Fokker–Planck Equation, Berlin: Springer-Verlag, 1989
31. Y. Kuramoto, Chemical Oscillations, Waves and Turbulence, Berlin: Springer-Verlag, 1984
32. Z. G. Zheng, G. Hu, and B. Hu, Phase slips and phase synchronization of coupled oscillators, *Phys. Rev. Lett.*, 1998, 81(24): 5318
33. Z. H. Liu, Y. C. Lai, and F. C. Hoppensteadt, Phase clustering and transition to phase synchronization in a large number of coupled nonlinear oscillators, *Phys. Rev. E*, 2001, 63(5): 055201 (R)
34. Y. Wu, J. H. Xiao, G. Hu, and M. Zhan, Synchronizing large number of nonidentical oscillators with small coupling, *Europhys. Lett.*, 2012, 97(4): 40005